European Journal of Pharmaceutical Sciences 172 (2022) 106137

Contents lists available at ScienceDirect

European Journal of Pharmaceutical Sciences

journal homepage: www.elsevier.com/locate/ejps

# Linear solvation energy relationships (LSERs) for robust prediction of partition coefficients between low density polyethylene and water. Part I: Experimental partition coefficients and model calibration

Thomas Egert [a,b,*], Horst-Christian Langowski [b,c]

[a] Boehringer Ingelheim Pharma GmbH & Co.KG, Ingelheim/Rhein, Germany
[b] Technical University of Munich, TUM School of Life Sciences Weihenstephan, Chair of Food Packaging Technology, Weihenstephaner Steig 22, Freising, 85354, Germany
[c] Fraunhofer Institute for Process Engineering and Packaging IVV, Giggenhauser Str. 35, Freising, 85354, Germany

ARTICLE INFO

*Keywords:*
Extractables to Leachables Correlation
Sorption to Polymers
Predicted Partition Coefficients LDPE/Water
Linear Solvation Energy Relationship (LSER)
Mass Transport Modeling (MTM)

ABSTRACT

When equilibrium of leaching is reached within a product's duty cycle, partition coefficients polymer/solution dictate the maximum accumulation of a leachable and thus, patient exposure by leachables. Yet, in the pharmaceutical and food industry, exposure estimates based on predictive modeling typically rely on coarse estimations of the partition coefficient, with accurate and robust models lacking. This first part of the study aimed to investigate linear solvation energy relationships (LSERs) as high performing models for the prediction of partition coefficients polymer/water. For this, partition coefficients between low density polyethylene (LDPE) and aqueous buffers for 159 compounds spanning a wide range of chemical diversity, molecular weight, vapor pressure, aqueous solubility and polarity (hydrophobicity) were determined and complimentary data collected from the literature (n=159, MW: 32 to 722, $\log K_{i,O/W}$: -0.72 to 8.61 and $\log K_{i,LDPE/W}$: -3.35 up to 8.36). The chemical space represented by this compounds set is considered indicative for the universe of compounds potentially leaching from plastics. Based on the dataset for the LDPE material purified by solvent extraction, a LSER model for partitioning between LDPE and water was calibrated to give: $\log K_{i,LDPE/W} = -0.529 + 1.098\,E_i - 1.557\,S_i - 2.991\,A_i - 4.617\,B_i + 3.886\,V_i$. The model was proven accurate and precise (n = 156, $R^2 = 0.991$, RMSE = 0.264). Further, it was demonstrated superior over a log-linear model fitted to the same data. Nonetheless, it could be shown that log-linear correlations against $\log K_{i,O/W}$ can be of value for the estimation of partition coefficients for nonpolar compounds exhibiting low hydrogen-bonding donor and/or acceptor propensity. For nonpolar compounds, the log - linear model was found as: $\log K_{i,LDPE/W} = 1.18 \log K_{i,O/W} - 1.33$ (n = 115, $R^2 = 0.985$, RMSE=0.313). In contrast, with mono-/bipolar compounds included into the regression data set, an only weak correlation was observed (n= 156, $R^2 = 0.930$, RMSE = 0.742) rendering the log-linear model of more limited value for polar compounds. Notably, sorption of polar compounds into pristine (non-purified) LDPE was found to be up to 0.3 log units lower than into purified LDPE. To identify maximum (i. e. worst-case) levels of leaching in support of chemical safety risk assessments on systems attaining equilibrium before end of shelf-life, it appears adequate to utilize LSER - calculated partition coefficients (in combination with solubility data) by ignoring any kinetical information.

## 1. INTRODUCTION AND BACKGROUND

Plastic materials still experience rising demand for use in manufacturing and packaging of medicinal products, their intermediates and medical devices as well (Freedonia, 2018; Smithers, 2019). When in contact with pharmaceutical preparations or human body compartments, they will unavoidably be involved in the distribution, i. e. leaching or sorption, of small molecules between phases. Here, patient exposure to potentially harmful substances leaching from plastics has become an issue of increasing regulatory scrutiny over the past two decades.

Several regulatory texts EMA, 2005; ISO, 2020; U.S. FDA, 1999; USP, <661>, 2015; USP <1663>, 2020; USP <1664>, 2020, along with

* Corresponding author: Thomas Egert, Boehringer Ingelheim GmbH & Pharma KG, Binger Straße 173, D-55216 Ingelheim/Rhein, +49 6131 77 97131
*E-mail address:* thomas.egert@boehringer-ingelheim.com (T. Egert).

https://doi.org/10.1016/j.ejps.2022.106137
Received 1 October 2021; Received in revised form 10 January 2022; Accepted 1 February 2022
Available online 9 February 2022

**Nomenclature**

*Symbols*

| | |
|---|---|
| C | Molar concentration |
| E, S, A, B, V, L | Abraham-type LSER solute descriptors |
| f | Volume fraction (0 - 1) |
| $\Delta G$ | Gibbs free energy (J $mol^{-1}$ $K^{-1)}$ |
| K | Volume-based molar partition coefficient (L/L) |
| R | Relative gas constant (J $mol^{-1}$ $K^{-1)}$ |
| S | Molar solubility limit |
| β | Phase ratio for two-phased partition system $K_{i,1/2}$ based on volume, for polymer and contacting medium: $\beta = V_{1=P}/V_{2=M}$ (-) |
| T | Temperature (K) |
| V | Phase volume (L) |

*Subscripts*

| | |
|---|---|
| LDPE | Low density polyethylene |
| M | (Contacting) Medium |
| O | Octanol phase |
| P | Polymer phase |
| PE | Polyethylene |
| W | Water (or aqueous) phase |
| tot | Total pool of leachable compound, mol |

*Superscripts*

| | |
|---|---|
| amorph | Amorphous fraction |
| C | Crystalline |
| eq | At equilibrium |
| 0 | Time zero/ initial |

best-practice industry recommendations (PQRI, 2006; BPOG, 2017) specify requirements to study the profile of compounds which can potentially be released from a material (extractables) and the resulting profile in a contacting (clinically relevant) medium (leachables). While the levels of leachables are decisive for patient exposure and the related toxicological assessment, special emphasis should be devoted to their qualitive and quantitative correlation to extractables. The underlying paradigm is that with the nature, composition and supply chain of a material well understood, knowledge about its constituents and their potential to leach can be leveraged to inform patient exposure and safety risk.

Further, for a long time (Crank, 1975; Fick, 1855), it has been established that small molecule mass transport (leaching) between well-separated, homogeneous and liquid-like phases is a physically foreseeable process. For many amorphous and semi-crystalline plastics used as primary contact material in the pharmaceutical- and food industry, the latter presents an appropriate assumption if the contact medium does not lead to penetration/swelling of the macromolecular structure.

By invoking suitable physical – and physicochemical models, the required key parameters, i. e. diffusion coefficients, solubility limits and partition coefficients can be estimated and the accumulation of leachables in a contacting medium , for example a drug solution, can be projected.

Along these lines, considerable research has been conducted in both the food - and pharmaceutical industry with several review articles available (Begley 2005; Franz 2005; Jenke 2011; Fang 2017; Piringer 2008). In the food industry, the related concept is termed 'Migration Modeling' and is officially recognized to estimate migration into food both in the EU and U.S. (EU 2011; U.S. FDA 2007)

More recently, research on the overall concept of mathematical- or predictive modeling has also been extended in support of material safety for pharmaceutical – and medical device applications (Jenke and Barge, 2014; Welle 2014; Egert 2018; Saylor et al.; 2019, Paudel 2020; Hauk et al.; 2021). However, as the industry approach with respect to studies on extractables and leachables is largely driven by experimentally-based, analytical protocols (Jenke, 2017), workflows for a chemical safety risk assessment yet typically neglect information on physicochemical factors dominating the distribution of compounds in the system under investigation.

The underlying process of small molecule mass transport, i. e. leaching from - and sorption to polymers, is kinetically governed by the mobility of the migrants in the polymer P, as expressed by the diffusion coefficient $D_{i,P}$ (with typically diffusion coefficients in polymer much lower than in the contacting medium M, i.e. $D_{i,P} \ll D_{i,M}$). However, thermodynamically, equilibrium concentrations are dictated by the partition coefficient, $K_{i,P/M}$, between polymer and the (clinically relevant contact) medium (CRM), rendering it a key parameter with respect to the accumulation of leachables and thus, ultimately, patient exposure. The molar partition coefficient $K_{i,P/M}$ is defined by the equilibrium concentrations of a migrant in the contacting polymer and media phases. For low concentrations of a neutral solute and applicable to well-separated, homogeneous and liquid-like phases involving a polymer, it can also be expressed by the differential solubilities $S_{i,P}$ and $S_{i,M}$ in both phases:

$$K_{i,P/M} = \frac{C_{i,P}^{eq}}{C_{i,M}^{eq}} \approx \frac{S_{i,P}}{S_{i,M}} \quad (1)$$

With: $C_{i,P}^{eq}$ equilibrium concentration in polymer, $C_{i,M}^{eq}$ equilibrium concentration in medium, $S_{i,P}$ : solubility limit in polymer, $S_{i,M}$ solubility limit in medium (all in molar concentrations). With amorphous polymers and elastomers potentially exhibiting high mobility by nature, i. e. high diffusion coefficients, equilibrium is often attained within a product's duty cycle, rendering mass transport to be controlled either by partitioning or limiting solubilities of the migrant.

However, depending on the specific makeup of polymer, contact medium composition, molecular structure and concentration of migrant, and as well, temperature and time of contact, realistic systems can deviate from idealized behavior (i.e. the situation of well-separated, homogeneous and liquid-like phases). Countercurrently to leaching, a certain degree of sorption of (organic) low molecular constituents from the contact medium to the polymer unavoidably occurs. Depending on the extent of this sorption (penetration) process, this might cause swelling of the macromolecular network and potentially coextraction of the migrant (Guazzotti, 2021; Kubicova, 2022; Kühne, 2021). Also, the polymer's heterogeneity and thereby, the migrant's accessibility might be affected (Feigenbaum, 2000) or is preventive for linear sorption on its own (Guo, 2012; Uber, 2019). As both effects typically lead to higherdiffusion and therefore overestimation of migration, they can also markedly alter the equilibrium polymer's sorption propensity and thereby partitioning behavior. The intrinsic partition coefficient given by Eq. 1 then requires replacement by an 'effective' partition coefficient, $K_{i,P/M}^{eff}$, for the realistic situation, accordingly. Note that such effective equilibrium partition coefficients might also strongly depend on temperature and thickness (geometry) of the polymer phase.

For an idealized system presuming equilibrium and starting from Eq. 1, one can express the fraction leached from the polymer $f_{i(leached)}$ by:

$$f_{i(leached)} = \frac{1}{(1 + K_{i,P/M}\,\beta)} \approx \frac{1}{\left(1 + \frac{S_{i,P}}{S_{i,M}}\,\beta\right)} \quad (2)$$

In Eq. 2, $\beta = V_P/V_M$ is the phase ratio where $V_P$ and $V_M$ represent the volumes of the polymer and contacting medium, respectively. With,

initially, the total pool $m_{i,tot}$ of migrant present in polymer only, i. e. the initial migrant mass $m^0_{i,P} = m_{i,tot}$, the equilibrium concentration of a leachable in medium, $C^{eq}_{i,M}$ results as:

$$C^{eq}_{i,M} = \frac{C^0_{i,P}}{1/\beta + K_{i,P/M}} \quad (3)$$

where $C^0_{i,P}$ is the initial concentration in polymer. With volumes of polymer and medium set, inspection of Eqs. 2 and 3 reveals the paramount importance of $K_{i,P/M}$ as dictating leachables accumulation in systems with high diffusivity. As many CRM are aqueous-based, knowledge of the partition coefficient polymer/water is of fundamental interest.

Experimental determination of $K_{i,P/M}$ is resource intensive and comes with several obstacles. Also, because of the vast number of combinations of chemicals, polymers and contacting media, the availability of experimental data is typically unlikely. Hence, general models for the estimation of $K_{i,P/M}$ with adequate accuracy and robustness are highly needed. Reliable estimates for partition coefficients, can, for example, be leveraged in studies on extractables and leachables facilitating a standardized approach of calculating worst-case leachables accumulation levels or serving as a plausibility check for experimental data.

In the food industry, officially recognized models for predicting migration suggest an only coarse classification of the migrant partition behavior by setting K to 1 (migrant well soluble in contact medium) or 1000 (migrant only sparingly soluble in contact medium), following some indication of hydrophobicity (Hoekstra, 2015). For improvement, several researchers have suggested the calibration of log-linear, Collander-type correlations (Collander, 1951), for example as based on the logarithm of aqueous solubility (Mercea et al., 2019) or to partitioning properties of an organic solvent/water system, typically octanol/water ($logK_{i,\ O/W}$) as a standard physicochemical property of general availability (Hayward et al., 1990). As such, log-linear correlations essentially represent a single-parameter linear free-energy relationships (spLFER), taking the form (Goss, 2003):

$$K_{i,P/M} = a \cdot logK_{i,O/W} + b \quad (4)$$

However, drawbacks of this approach have been abundantly documented, the most significant being the fact that octanol/water cannot serve as a system which properly represents all relevant molecular interactions a solute is exposed to (Goss and Schwarzenbach, 2001; Goss, 2003; Josefsson et al., 2015; Pintado-Herrera et al., 2016).

### 1.1. Abraham-type LSERs

Poly-parameter linear free-energy relationships (ppLFERs) have been designed to mitigate this problem (Abraham et al., 1982; Taft et al., 1985) and, for well over two decades, have been mainly utilized in solution - and analytical chemistry, environmental - and agrochemistry and as well as in the pharmaceutical field to characterize free-energy related processes, notably, partitioning. As such, the natural logarithm of a partition coefficients is linearly related to the Gibbs free energy of transfer of a solute's total pool between phases, accordingly for partitioning involving polymers:

$$\Delta G_i = -RT \ln K_{i,P/M} + \ln(constant) \quad (5)$$

ppLFERs have the potential to predict and provide chemical insight into processes dependent on the equilibrium transfer or the rate of transfer of a compound (solute) between gas-liquid, liquid-liquid, liquid-solid, and more complex phases, for example, polymers (Goss, 2011).

Amongst various types of ppLFERs reported, Abraham-type linear solvation energy relationships (LSERs), are particularly useful (Abraham, 1993). Basically, a free-energy related solute property, SP, (equal to $(\Delta G_i - const)/RT$, e. g. the equilibrium partition coefficient $logK_{i,j/k}$ between phases j and k, can be correlated to five carefully selected and quantitatively scaled solute descriptors encoding for the potential strength of a molecule to undergo interactions with a surrounding phase:

Two condensed phases (EV-model):

$$logK_{i,j/k} = c + eE_i + sS_i + aA_i + bB_i + vV_i \quad (6)$$

Gas/condensed phase (EL-model):

$$logK_{i,j/k} = c + eE_i + sS_i + aA_i + bB_i + lL_i \quad (7)$$

Eq. 6 is used for the transfer of a compound between condensed phases such as octanol and water ($logK_{i,\ O/W}$) or other systems of solvent partitioning, whereas Eq. 7 applies to transfer between a gas- and a condensed phase such as air/water ($logK_{i,\ A/W}$) or air/solvent (polymer), respectively. For both situations and giving an equivalent quality of fit, Goss (Goss, 2005) has provided another equation with only $vV_i$ and $lL_i$ as non-specific terms and improved predictability for fluorinated compounds and siloxanes (Endo and Goss, 2014b), respectively:

Universal phases (VL-model):

$$logK_{i,j/k} = c + sS_i + aA_i + bB_i + vV_i + lL_i \quad (8)$$

The five descriptor pairs quantify the molecular interactions that govern the partition process: non-specific van der Waals interactions and cavity formation ($vV_i$, $eE_i$ or $lL_i$), and specific polar interactions, i. e. dipolarity/polarizability ($sS_i$) and hydrogen-bond interactions ($aA_i$ and $bB_i$ ). The upper case letters in Eqs. 6, 7 and 8 denote the solute descriptors as follows: $\mathbf{E_i}$: excess molar refraction in units of $(cm^3mol^{-1})/10$, $S_i$: dipolarity/polarizability, $A_i$: solute hydrogen (H)-bond acidity, $B_i$: solute H-bond basicity, $V_i$: McGowan characteristic molar volume in units of $(cm^3\ mol^{-1})/100$ (Abraham and McGowan, 1987), and $L_i$: logarithmic hexadecane/air partitioning constant, respectively.

The lower case regression coefficients and regression constant (termed phase descriptors or system parameters) e, s, a, b, v, l and c in Eqs. (6) to (8) are obtained by multiple linear (MLR) regression of experimental solute properties (e. g. partition coefficient data) for a specific biphasic system. The regression coefficients and constants reflect the differential properties (or differential potential interactions) the solubilizing phases can undergo. Several excellent reviews exist and cover the subtleties and general applications of LSERs (Abraham et al., 2004; Endo and Goss, 2014a; Poole et al., 2009; Vitha and Carr, 2006).

Experimental solute descriptors for some thousands chemicals as well as system parameters for solvent-, technical- and biological systems can be conveniently extracted from a free but curated, web database (Ulrich et al., 2017). Upon submitting the compound's SMILES code, the website also offers a quantitative structure property relationship algorithm (QSPR) for estimation of solute descriptors, thus enabling calculations for any known chemical structure.

For "liquid-like", i.e. highly amorphous polymers, the type of molecular interaction with compounds spanning the universe of extractables is hypothesized as similar to sorption into any liquid phase. Consequently, partitioning between polymers exhibiting linear sorption isotherms at relevant concentrations and an non-penetrating, aqueous phase is expected to be adequately fitted by free energy of transfer - based models (LSERs). LSERs have yet not been explored for the estimation of partition coefficients utilized in the safety evaluation of pharmaceutical - and food contact materials. Notwithstanding, a few reports on LSER models trained by chemically diverse compound sets and characterizing sorption from water to polymers in use for environmental sampling, namely polydimethylsiloxane (PDMS), polyacrylate (PA) and polyoxymethylene (POM) exist (Sprunger et al., 2007, Endo et al., 2011a; Endo et al., 2011b). Due to the wide use of polyolefins in pharmaceutical applications, an experimentally trained LSER model with a broad application domain for polyolefin type materials would be of high value but is currently unavailable.

### 1.2. Study aim

In this part I of the study, it is aimed to obtain thoroughly determined partition coefficients between low density polyethylene (LDPE) and water for a broad set of compounds spanning a wide range of chemical diversity, molecular weight, vapor pressure, aqueous solubility and polarity (hydrophobicity). LDPE, representative for the family of polyolefines, is a material of particular interest for pharmaceutical applications.

Further on, based on these data, this work aims to establish a quantitative model that can accurately estimate $K_{i,LDPE/W}$ for a broad range of compounds. To this end, we introduce and explore Abraham-type LSERs as a user-friendly concept for the prediction of the partition behavior of virtually any neutral organic compound. Two types of LSER models will be calibrated and their performance and statistics characterized and compared to a log-linear correlation (spLFER) to $\log K_{i,O/W}$ by accounting for the hydrogen-bonding capacity of compounds.

In part II of the study, further validation of the LSER-models and their comparison to other models and data from the literature will be reported (Egert et al., 2022).

## 2. EXPERIMENTAL

### 2.1. Materials

#### 2.1.1. LDPE film

LDPE films made of Lupolen 3020 D (thickness 50 and 200 μm) were obtained from Polifilm Extrusion GmbH, Germany to represent a type of polyethylene widely used for pharmaceutical applications.

Measurements were conducted on the pristine material as received (LDPEpris) and after purification as well (LDPE). While pristine (non-purified) material represents the standard use case, partition coefficients from the literature in most cases originate from studies on partition behavior of purified LDPE material as employed in environmental passive sampling. Therefore, to align pretreatment (purification) of the materials submitted to the experiments, the LDPE film for the batch experiments in this study was extracted as follows: LDPE films were cut into strips and immersed first in n-hexane, and then in methanol followed by water for at least 1 day, each. Afterwards, solvent residues were allowed to evaporate at 60°C for 2 days in a drying cabinet.

On this basis, the weight loss from the LDPE film was, gravimetrically found to be 0.67 % w/w and the residue after evaporation of the n-hexane extract was gravimetrically found as 0.61 % w/w. The extracted matter was of greasy consistence and by qualitative GC/MS-profiling characterized to consist mainly of oligomers originating from the polymerization process and termed polyolefin saturated hydrocarbons (POSH) (Biedermann-Brem et al., 2012). By means of gas chromatography (GC), this extracted matter was detected as an "unresolved hump" which corresponded to an elution time-range of linear hydrocarbons between n-C20 to n-C46 with a maximum around n-C36. (see section 1 and Fig. SI 1 of the supporting information (SI)). As the crystallinity of the film could not be retrieved from available certification, it was adopted from literature data for generic LDPE as $X^{C}_{LDPE} = 35$ % v/v (Lützow et al., 1999). The volume of the amorphous LDPE phase is then obtained from the total volume according to:

$$V^{amorph}_{LDPE} = V^{tot}_{LDPE}\left(1 - X^{C}_{LDPE}\right) \quad (9)$$

where $V^{amorph}_{LDPE}$: amorphous volume of LDPE film (sample), $V^{tot}_{LDPE}$: total experimental volume of LDPE film (sample), $X^{C}_{LDPE}$: crystallinity attributed to LDPE sample.

#### 2.1.2. Silicone (PDMS) film

A silicone (polydimethyl siloxane (PDMS)) film was prepared in-house at a thickness of 367 μm by using a two-component formulation (Silastic MDX 4120, Dow Corning), obtained from Biesterfeld GmbH, Hamburg, Germany. The film was pre-extracted similarly to the LDPE film.

#### 2.1.3. Test solute set

Test solutes for our own measurements were carefully selected based on the availability of experimentally determined solute descriptors and to cover a wide range of molecular weight and diverse chemical structures (Table 2). These compounds were obtained from different providers with a minimum purity of 95%. Organic solvents and inorganic salts were purchased from Merck and were of analytical, GC or LC grade. Water for all experiments was purified with a Milli-Q A10 Ultrapure Water Purification System (Millipore, Eschborn, Germany). Various buffer solutions were prepared at pH values of 2.0, 4.0, 6,0 and 8.0 (Table SI 1 in SI). To prevent microbial activity in the test system, sodium azide ($NaN_3$) at50 mg/L was added to all buffer solutions.

The set of test solutes for batch equilibrium sorption experiments is provided in Table SI 2 along with experimentally determined LSER solute descriptors.

### 2.2. Methods

#### 2.2.1. Batch equilibrium sorption experiments to determine $K_{i,LDPE/W}$

$K_{i,LDPE/W}$ was determined by batch equilibrium sorption experiments utilizing buffered aqueous solutions. LDPE film of 200 μm thickness was cut into strips of 2 cm width with a scalpel. The strips were further longitudinally cleaved to support an uneven surface after crinkling which efficiently avoided adhesion to the container walls. 10 to 500 mg of LDPE (density 0.927 g/cm$^3$) were accurately weighed into glass containers of different volumes. The containers then received aqueous buffer solutions at volumes of 4.0 mL up to 60.0 mL and were subsequently spiked with a cocktail of 6-10 compounds in methanol. Spiked solute amounts were designed to avoid exceedance of the solute solubility limit in the aqueous solution after equilibration. The fraction of methanol in the buffer solution did not exceed 0.25 % (v/v) to avoid a cosolvency effect (McPhedran et al., 2012). Also, loading of the polymer phase was always below 2 g/L of LDPE with no expected impact on the sorption characteristics of LDPE. Following previous reports (Belles et al., 2016; Hüffer and Hofmann, 2016), linear sorption isotherms were precluded and therefore only one concentration level was tested per batch experiment. Three replicates were prepared for each solute mixture. The vials were immediately sealed with PTFE/silicon-lined crimp caps. Vials hosting non-volatile test compounds were sealed by aluminium-coated/silicon-lined screw caps.

The volume ratio of the phases, i. e. polymer and aqueous buffer solution was adjusted to achieve sorption rates of the total amount of solute spiked between 5% and 95 % where possible. However, with striving for a maximal range of experimental $\log K_{i,LDPE/W}$, and under the phase-ratio restrictions of the batch equilibrium sorption method used, this range could not be realized at the lower ($\log K_{i,LDPE/W} < 0$) and higher end ($\log K_{i,LDPE/W} > 4$) of the solute $\log K_{i,LDPE/W}$ scale. Consequently, at these extremes the resulting equilibrium concentrations either in the solution or polymer were, at a minimum, required to range at or above the quantitation limit of the analytical procedure.

To enhance equilibration, batches were stored for 21 days at 40°C in a drying cabinet and manually agitated once a working day. The vials were then agitated horizontally at 25 ± 2°C for another 14 days on a shaker. Test compounds in the cocktails were carefully organized to fulfill several criteria: (i) projected $\log K_{i,LDPE/W}$ of test solutes within a maximum of 1.5 units, (ii) all test solutes prevalently exist in their neutral form at the pH of the chosen buffer and (iii) no analyte coelution in the analytical quantitation method (relevant to LC/UV).

Each batch experiment contained additional triplicate samples of LDPE film of 50 μm thickness, which are expected to result in distinctly

faster equilibration times then the 200 μm films used for calculation of partition coefficients. Triplicate experimental determination of $\log K_{i,LDPE/W}$ with a relative deviation of the means < 5% between the two film thicknesses was considered evidence, that equilibrium had been attained. Blank control samples and spiked blank sample lacking the polymer were measured in parallel to monitor cross-contamination and compound losses from the system.

Table 1 provides an overview of experimental batches for equilibrium sorption including spiked amounts, phase volumes as well as preparation and analysis of each phase.

### 2.2.2. Analysis of LDPE strip

After equilibration, LDPE films were retrieved from the solution using solvent-rinsed stainless-steel tweezers, immediately wiped with a clean, lint-free tissue to remove adhering solution and transferred to a glass vial for organic solvent extraction. The weight of the polymer was recorded and the extraction solvent was immediately dispensed into the extraction vial and sealed. Dichloromethane was used for analysis of the extract by GC/MS and acetone was used for analysis by HPLC/UV. Static sealed vessel extraction at 40°C in a drying cabined for 24 hours was followed by horizontal shaking of the vial for another 24 hours at room temperature. Recovery samples for the solvent extraction process were prepared in parallel and the extraction recoveries (determined at mostly > 90%) were used for result calculation.

Volatile- (VOC) and semi-volatile (SVOC) compounds in the back-extracted LDPE strips samples were quantified by GC/MS/MS. After extraction of the strips as indicated in Table 1, 1.0 mL of the final extract were transferred to a GC vial and 100 μL of an internal standard solution containing toluene-$d_8$, chlorobenzene-$d_5$, 1,1,2-trichloropropane and 3-nonanol at nominally 100 μg/ml in dichloromethane were added.

Non-volatile compounds (NVOC) were quantified by LC/UV. 1.0 mL of the final extract according to Table 1 was transferred to a LC vial and 100 μL of an internal standard solution containing 2-nitroanisole and acenaphthene-$d_{10}$ at nominally 100 μg/ml in acetone were added.

### 2.2.3. Analysis of aqueous batch sorption samples

Equilibrium concentration levels of the test solutes in the aqueous phase of the batch sorption samples were measured by following a process adapted to the spiked solute cocktails as containing VOC, SVOC or NVOC.

Volatile test compounds were analyzed by Headspace-GC/MS. For this, aliquots of the aqueous phase from batch samples were transferred to a 22 mL headspace vial and 100 μL of an internal standard solution containing toluene-$d_8$, chlorobenzene-$d_5$, 1,1,2-trichloropropane and 3-nonanol at nominally 10 μg/ml in dimethylformamide were added. After equilibration, the headspace of the vial was analysed and solute concentrations calculated against multilevel calibration curves from freshly prepared standard solutions by the internal standard method.

### 2.2.4. HS-GC/MS measurements

A Perkin Elmer Turbomatrix 40 Headspace Sampler was coupled to an Agilent 7890A GC / Agilent 7975 C Inert XL MSD. The transferline from the sampler was directly coupled to the analytical column, bypassing the GC-injector. Carrier gas was supplied by the headspace sampler (Helium 99.999 at 60 kPa). Sample equilibration was at 80°C for 30 min. Transfer line temperature was 120°C and the injection needle temperature was 125°C. Injection pressurization time was 3 min with a dwell time of 0.2 min and 0.02 – 0.04 min injection time.

GC-Injector temperature was set to 120°C. Analytical column: Restek Rxi 624SilMS, 30m, 0.32 mmID, 1.8μm df (Restek, Germany). Oven program: 40°C – 2 min – 10K/min – 100°C – 0 min – 15K/min – 160°C - 0 min – 20K/min – 240°C - 0 min – 30K/min – 270°C – 1 min (total 18 min). Detection: El 70 eV, transfer line temperature 280°C, Ion source: 230°C, Analyzer temperature: 150°C. No solvent delay was applied. Analyzer was operated in single ion monitoring mode (SIM) with 2 - 3 ions per compound at high resolution at dwell times between 25 and 80 ms. Electron multiplier offset was 200 V. For data acquisition, Agilent Mass Hunter GC/MS Aquisition B.07.03 (2129) was used.

Semi Volatile compounds were back-extracted from the equilibrated aqueous phase by n-hexane and quantified by GC/MS/MS as specified in Table 1. For instrumental analysis, 1.0 mL of the final extract were transferred to a 2 mL GC vial and 100 μL of an internal standard solution containing toluene-$d_8$, chlorobenzene-$d_5$, 1,1,2-trichloropropane and 3-nonanol at nominally 100 μg/ml in dichloromethane at approximately 100 μg/mL, were added.

### 2.2.5. Instrumental conditions for GC/MSMS

GC/MS/MS analysis was performed using an Agilent 7890A GC coupled to a 7001 B Triple Quadrupole Detector equipped with a multimode injection (MMI) system. Operating conditions were as follows:

Injector temperature 280°C Injection volume 0.5 – 0.75 μL. Split ratio 1:10. Analytical column: Restek Rxi 624SilMS, 30m, 0.32 mm ID, 1.8 μm df (Restek, Germany). Carrier gas: Helium, purity 99.999% at 1.7 mL/min (constant flow mode). Oven program: 40°C – 2 min – 10K/min – 100°C – 0 min – 15K/min – 160°C - 0 min – 20K/min – 240°C - 0 min –

**Table 1**
Preparation scheme for batch equilibrium sorption samples

| Batch | Nominal amount spiked (μg) | Polymer phase LDPE (mL) | Sample prep [b] | Analysis | Aqueous phase Buffer (mL) | Sample prep [b] | Analysis |
|---|---|---|---|---|---|---|---|
| VOC No 1 | 500 | 0.5 | Ex DCM | GC/MS/MS | 8 | na | HS-GC/MS |
| VOC No 2 | 200 | 0.5 | Ex DCM | GC/MS/MS | 8 | na | HS-GC/MS |
| VOC No 3 | 100 | 0.5 | Ex DCM | GC/MS/MS | 8 | na | HS-GC/MS |
| VOC No 4 | 37.5 | 0.2 | Ex DCM | GC/MS/MS | 8 | na | HS-GC/MS |
| VOC No 5 | 25 | 0.05 | Ex DCM | GC/MS/MS | 20 | na | HS-GC/MS |
| SVOC No 1 | 100 | 0.25 | Ex DCM | GC/MS/MS | 4 | Ex DCM | GC/MS/MS |
| NVOC No 1 [a] | n/a | n/a | n/a | LC/UV | n/a | n/a | LC/UV |
| NVOC No 2 | 65 | 0.5 | Ex ACT | LC/UV | 4 | DI LC | LC/UV |
| NVOC No 3 | 60 | 0.1 | Ex ACT | LC/UV | 4 | DI LC | LC/UV |
| NVOC No 4 | 25 | 0.05 | Ex ACT | LC/UV | 4 | DI LC | LC/UV |
| NVOC No 5 | 25 | 0.04 | Ex ACT | LC/UV | 40 | Ex nHex | LC/UV |
| NVOC No 6 | 10 | 0.025 | Ex ACT | LC/UV | 60 | Ex nHex | LC/UV |
| NVOC No 7 | 10 | 0.01 | Ex ACT | LC/UV | 60 | Ex nHex | LC/UV |

[a] batch results not evaluated due to insufficient data quality
[b] Sample preparation procedure:
Ex ACT, Extraction with acetone (sealed vessel)
Ex DCM, Extraction with dichloromethane (sealed vessel)
Ex nHex, Extraction with n-hexane (sealed vessel)
DI LC, Direct injection into LC

30K/min – 320°C – 1 min (Total 19.667 min). Transfer line temperature 300°C. Detection: El 70 eV, Ion source temperature 280°C, Quadrupol temperature: 150°C. Solvent delay: adjusted to retention time of early eluting targets. Analyzer was operated in multi reaction mode (MRM) with two transitions monitored for each target compound at dwell times between 10 and 100 ms. Collision energies were optimized for each transition in a range from 0 – 60 at steps of 5. Electron multiplier offset was 200 V.

Non-volatile test compounds were analyzed after liquid/liquid extraction of an aliquot from the equilibrated aqueous phase (Table 1). For analysis by HPLC/UV, 1.0 mL of the final extract were transferred to a 2 mL LC vial and 100 µL of an internal standard solution containing 2-nitroanisole and acenaphthene-$d_{10}$ at nominally 100 µg/ml in acetone, were added.

#### 2.2.6. Instrumental conditions for LC/UV

An Agilent 1200 series LC/UV system was used. 8 µL of the sample was injected onto a reversed phase separation column (Phenomenex Synergi 2.5 µ Hydro-RP 100 A 100 × 3.0mm 2.5 µm Cat 00-4387-40) held at 40°C. The mobile phase was a gradient made of monobasic potassium phosphate at 10 mM adjusted to a pH of 2.0 (mobile phase A) and acetonitrile (phase B). The gradient profile for acetonitrile (mobile phase B) was as follows: Initial flow rate: 0.8 mL/min: 6%, 2.0 min: 6%, 6.0 min: 42%, 8.0 min: flow rate 0.9 mL/min, 60%, 18 min:: flow rate 1.7 mL/min 80%, 20 min:: flow rate 1.9 mL/min 100%, 24 min: flow rate 1.9 mL/min 100%.

Target compounds were detected at or close to their absorption maximum. The reference wavelength was 550 nm at 10 nm bandwidth.

Calibration curves at a minimum of 5 levels were generated with either a linear or quadratic fit and 1/y or $1/y^2$ weighting, respectively. The calibration curves spanned a concentration from the instrumental detection level up to a level which adequately covered the maximum theoretical concentration projected for the test solutes in the aqueous phase.

#### 2.2.7. Calculations

The measurement of accurate and precise partition coefficients between polymers and aqueous solutions for a large number of compounds comes with challenges, especially at the lower and upper ends of the $\log K_{i,Polymer/W}$ – scale, requiring quantitation of trace-level amounts either in the polymer or solution, respectively. Therefore, measures to support good data quality were taken as follows:

$\log K_{i,LDPE/W}$ values obtained from equilibrium concentrations as measured in both phases:

$$\log K_{i,LDPE/W} = \log\left(\frac{C^{eq}_{i,LDPE}}{C^{eq}_{i,W}}\right) \quad (10)$$

A mass balance calculation was carried out for each experiment. In principle, as concentrations are measured in both phases, $\log K_{i,LDPE/W}$ can be obtained even with mass losses during the experiment (for example volatilization, glassware sorption, degradation, transformation). However, to ensure good data quality, only results with mass balances ≥ 60 % (SVOC and NVOC) and ≥ 50 % (VOC) as related to the initially spiked amount were considered for model calibration. Aqueous solubility data for all solutes were collected prior to the experiments. Phase ratios and spiked amounts for the batch experiments were carefully adjusted to ensure equilibrium concentrations aligned to the working range of the analytical procedure as well as aqueous levels well below the test solute's solubility limits.

Concurrent samples deploying a polydimethylsiloxane (PDMS) film were analyzed under identical conditions and measured $\log K_{i,PDMS/W}$ were compared to predicted data using a model calibrated by (Sprunger et al., 2007). A high consistency (mean deviation of 0.2 log units for test solutes listed in Table 2) between measured and predicted values was considered additional proof for the validity of the total batch experimental procedure.

#### 2.2.8. Literature data for $\log K_{i,LDPE/W}$

This study's experimental setup did not include compounds of very high hydrophobicity ($\log K_{i,O/W} > 6$). To extend the model calibration domain it therefore appeared beneficial to expand the test solute set by inclusion of further experimental data for $\log K_{i,LDPE/W}$ from the literature. Literature data available were critically assessed to fulfill certain quality criteria:

Proof that equilibrium had been reached, consistency to values from other researchers, if applicable, availability of detailed experimental conditions, mass balances, experimental setup ensuring that equilibrium levels do not exceed solubility limits of solutes. Also, the identity of the polymer and the equilibration temperature was required to be specified.

Based on this, compilations by Liu (Liu et al., 2017) and Belles (Belles et al., 2016) were found to provide appropriate data for the extension of the data set measured in this study.

### 2.3. Data sets, models, and statistics

To facilitate comparison of performance between log-linear correlations to $K_{i,O/W}$ and LSERs, the following models for projection of $\log K_{i,LDPE/W}$ were calibrated:

#### 2.3.1. spLFER (log-linear) model

A simple least-squares linear regression equation representing a spLFER according to Eq. 4 was fitted to the experimental data. Here, it was aimed to deploy a possibly reliable set of $\log K_{i,O/W}$ data. Experimental values for $\log K_{i,O/W}$ were preferred over predicted values, where available, and were taken either from (Reaxys®) or from (EPI SuiteTM v4.11). Where no experimental value for $\log K_{i,O/W}$ could be identified, predicted values from different prediction tools were averaged. All $\log K_{i,O/W}$ values used are listed in Table SI 2 of the SI including indication of their source. The quality of fit of models obtained was characterized by an analysis of variance (ANOVA).

#### 2.3.2. ppLFER (LSER) model

LSER equations were calculated by means of a multiple linear regression (MLR) algorithm as implemented in the Excel® Solver and/or SigmaPlot V.14. An EV-model according Eq. 6 and as well a VL-model according Eq. 8, respectively, were calibrated, the latter for use in part II of this study. Statistics for the characterization of the LSER models constructed by means of MLR include number of observations (n), root mean squared error (RMSE) coefficient of determination ($R^2$) and Fisher's test value (F). Also, multicollinearity of the solutes descriptor sets was assessed with results summarized in the supporting information (Endo and Goss, 2014a).

## 3. RESULTS AND DISCUSSION

### 3.1. Probe solute set – structures, properties, solute descriptors and measured data

Fulfilling the specified quality criteria, 82 partition coefficients for both purified LDPE ($\log K_{i,LDPE/W}$) and pristine LDPE ($\log K_{i,LDPEpris/W}$) at 25°C were measured and are listed in Table 2. These data were complemented by further 77 values from 71 additional compounds for $\log K_{i,LDPE/W}$ (near 25°C) from the literature (Table 3).

The literature data set predominantly comprises more hydrophobic compounds ($\log K_{i,O/W}$ for most compounds > 4). Due to their origin from environmental studies, these compounds mainly represent polynuclear hydrocarbons (PNA), alkylated PNA, polychlorinated biphenyls (PCB), brominated diphenylethers (BDE) and alkylbenzenes amongst some others. Data were primarily taken from (Liu et al., 2017) and were thoroughly reviewed by the authors to be in good agreement with values

**Table 2**
Measured partition coefficients for purified LDPE ($\log K_{i,LDPE/W}$) and pristine LDPE ($\log K_{i,LDPEpris/W}$) near 25°C from this study ($L_{Water}$ / $L_{LDPE}$)

| ID | CAS | Compound | Measured $\log \mathbf{K}_{i,LDPE/W}$(1) | SD | LSER[b] calc $\log \mathbf{K}_{i,LDPE/W}$ (2) | Diff (2) – (1) | Measured $\log \mathbf{K}_{i,LDPEpris/W}$(3) | SD | Diff (3) – (1) |
|---|---|---|---|---|---|---|---|---|---|
| 1 | 80-62-6 | Methyl methacrylate | 0.12 | 0.00 | 0.20 | 0.08 | 0.13 | 0.01 | 0.01 |
| 2 | 140-88-5 | Ethyl acrylate | -0.10 | 0.01 | 0.05 | 0.15 | -0.08 | 0.03 | 0.02 |
| 3 | 97-88-1 | n-Butyl methacrylate | 1.81 | 0.03 | 1.57 | -0.24 | 1.77 | 0.02 | -0.04 |
| 4 | 67-56-1 | Methanol | -3.35 | 0.13 | -3.17 | 0.18 | -3.61 | 0.30 | -0.26 |
| 5 | 64-17-5 | Ethanol | -2.64 | 0.21 | -2.49 | 0.15 | -2.94 | 0.29 | -0.30 |
| 6 | 75-65-0 | tert.-Butanol | -1.84 | 0.01 | -1.66 | 0.18 | -2.04 | 0.00 | -0.20 |
| 7 | 100-51-6 | Benzyl alcohol | -1.42 | 0.01 | -1.02 | 0.40 | -1.54 | 0.04 | -0.12 |
| 8 | 589-18-4 | 4-Methylbenzyl alcohol | -0.90 | 0.01 | -0.65 | 0.25 | -1.00 | 0.02 | -0.10 |
| 9 | 597-76-2 | 3-ethyl-3-hexanol | 0.46 | 0.01 | 0.56 | 0.10 | 0.37 | 0.03 | -0.09 |
| 10 | 143-08-8 | 1-Nonanol | 1.05 | 0.01 | 1.28 | 0.23 | 1.00 | 0.01 | -0.05 |
| 11 | 90-15-3 | 1-Naphthol | 0.26 | 0.01 | 0.42 | 0.16 | 0.21 | 0.01 | -0.05 |
| 12 | 98-55-5 | alpha-Terpineol | 0.78 | 0.01 | 0.83 | 0.05 | 0.67 | 0.02 | -0.11 |
| 13 | 89-78-1 | dl-Menthol | 1.10 | 0.01 | 1.47 | 0.37 | 1.03 | 0.01 | -0.07 |
| 14 | 123-72-8 | Butyraldehyde[b] | 0.13 | 0.07 | -0.74 | -0.87 | -0.79 | 0.07 | -0.92 |
| 15 | 66-25-1 | Hexanal [b] | 1.35 | 0.06 | 0.32 | -1.03 | 0.56 | 0.05 | -0.79 |
| 16 | 100-52-7 | Benzaldehyde | 0.25 | 0.05 | 0.41 | 0.16 | 0.25 | 0.05 | 0.00 |
| 17 | 124-19-6 | Nonanal [b] | 2.96 | 0.02 | 1.96 | -1.00 | 2.48 | 0.02 | -0.48 |
| 18 | 108-88-3 | Toluene | 2.10 | 0.08 | 2.00 | -0.10 | 1.95 | 0.08 | -0.15 |
| 19 | 108-90-7 | Chlorobenzene | 2.08 | 0.01 | 2.19 | 0.11 | 2.07 | 0.02 | -0.01 |
| 20 | 95-49-8 | 2-Chlorotoluene | 2.68 | 0.00 | 2.78 | 0.10 | 2.68 | 0.10 | 0.00 |
| 21 | 591-50-4 | Iodobenzene | 2.56 | 0.04 | 2.74 | 0.18 | 2.57 | 0.01 | 0.01 |
| 22 | 141-78-6 | Ethyl acetate | -0.65 | 0.01 | -0.55 | 0.10 | -0.72 | 0.02 | -0.07 |
| 23 | 123-92-2 | Isoamylacetate | 1.00 | 0.02 | 1.01 | 0.01 | 0.97 | 0.02 | -0.03 |
| 24 | 123-66-0 | Ethyl hexanoate | 1.71 | 0.04 | 1.62 | -0.09 | 1.70 | 0.02 | -0.01 |
| 25 | 119-36-8 | Methyl salicylate | 1.48 | 0.01 | 1.28 | -0.20 | 1.47 | 0.01 | -0.01 |
| 26 | 94-26-8 | Butyl-hydroxybenzoate | 0.04 | 0.01 | 0.21 | 0.17 | -0.07 | 0.03 | -0.11 |
| 27 | 109-99-9 | Tetrahydrofuran | -0.85 | 0.01 | -0.82 | 0.03 | -0.92 | 0.02 | -0.07 |
| 28 | 60-29-7 | Diethyl Ether | -0.31 | 0.01 | -0.08 | 0.23 | -0.30 | 0.00 | 0.01 |
| 29 | 123-91-1 | 1,4-Dioxane | -1.39 | 0.01 | -1.64 | -0.25 | -1.47 | 0.02 | -0.08 |
| 30 | 470-82-6 | Eucalyptol | 1.34 | 0.01 | 1.15 | -0.19 | 1.28 | 0.01 | -0.06 |
| 31 | 2043-47-2 | FTOH 4:2 | -0.11 | 0.03 | 0.42 | 0.53 | -0.26 | 0.03 | -0.15 |
| 32 | 647-42-7 | FTOH 6:2 | 1.32 | 0.16 | 1.72 | 0.40 | 1.06 | 0.04 | -0.26 |
| 33 | 110-80-5 | 2-Ethoxyethanol | -2.90 | 0.17 | -2.70 | 0.20 | -2.93 | 0.46 | -0.03 |
| 34 | 109-66-0 | Pentane | 2.86 | 0.04 | 2.63 | -0.23 | 2.88 | 0.13 | 0.02 |
| 35 | 628-71-7 | 1-Heptyne | 2.40 | 0.02 | 2.36 | -0.04 | 2.40 | — | 0.00 |
| 36 | 5989-54-8 | S(-)-Limonene | 3.85 | 0.05 | 3.74 | -0.11 | 3.84 | 0.02 | -0.01 |
| 37 | 76-22-2 | Camphor | 1.05 | 0.01 | 0.78 | -0.27 | 1.00 | 0.01 | -0.05 |
| 38 | 109-69-3 | Chlorobutane | 1.75 | 0.01 | 1.71 | -0.04 | 1.77 | — | 0.02 |
| 39 | 79-01-6 | Trichloroethylene | 1.78 | 0.01 | 1.87 | 0.09 | 1.79 | 0.11 | 0.01 |
| 40 | 107-04-0 | 1-Bromo-2-chloroethane | 0.81 | 0.00 | 0.97 | 0.16 | 0.85 | 0.01 | 0.04 |
| 41 | 96-18-4 | 1,2,3-Trichloropropane | 1.14 | 0.01 | 1.04 | -0.10 | 1.16 | 0.01 | 0.02 |
| 42 | 127-18-4 | Tetrachloroethene | 2.65 | 0.00 | 2.74 | 0.09 | 2.66 | 0.10 | 0.01 |
| 43 | 78-93-3 | Methyl ethyl ketone | -0.86 | 0.01 | -1.11 | -0.25 | -0.93 | 0.03 | -0.07 |
| 44 | 120-92-3 | Cyclopentanone | -0.91 | 0.01 | -1.06 | -0.15 | -0.97 | 0.01 | -0.06 |
| 45 | 591-78-6 | 2-Hexanone | 0.13 | 0.01 | -0.02 | -0.15 | 0.08 | 0.02 | -0.05 |
| 46 | 111-13-7 | 2-Octanone | 1.27 | 0.01 | 1.04 | -0.23 | 1.21 | 0.01 | -0.06 |
| 47 | 107-07-3 | 2-Chloroethanol | -2.06 | 0.01 | -2.80 | -0.74 | -2.14 | 0.06 | -0.08 |
| 48 | 110-02-1 | Thiophene | 1.06 | 0.01 | 1.14 | 0.08 | 1.10 | 0.00 | 0.04 |
| 49 | 110-81-6 | Diethyl disulfide | 2.16 | 0.03 | 2.00 | -0.16 | 2.10 | 0.02 | -0.06 |
| 50 | 103-84-4 | Acetanilide | -2.00 | 0.02 | -1.89 | 0.11 | -2.27 | 0.04 | -0.27 |
| 51 | 95-16-9 | Benzothiazole | 0.66 | 0.01 | 1.14 | 0.48 | 0.65 | 0.02 | -0.01 |
| 52 | 1193-82-4 | Methylphenyl sulfoxide | -1.44 | 0.04 | -2.13 | -0.69 | -1.71 | 0.08 | -0.27 |
| 53 | 100-06-1 | Acetanisole | 0.27 | 0.01 | 0.29 | 0.02 | 0.25 | 0.01 | -0.02 |
| 54 | 94-09-7 | Ethyl 4-aminobenzoate | -0.62 | 0.01 | -0.33 | 0.29 | -0.72 | 0.02 | -0.10 |
| 55 | 86-74-8 | Carbazole | 2.00 | 0.02 | 2.52 | 0.52 | 1.93 | 0.01 | -0.07 |
| 56 | 119-61-9 | Benzophenone | 1.99 | 0.01 | 2.17 | 0.18 | 1.98 | 0.01 | -0.01 |
| 57 | 132-65-0 | Dibenzothiophene | 4.02 | 0.02 | 4.11 | 0.09 | 3.98 | 0.10 | -0.04 |
| 58 | 94-25-7 | Butyl 4-aminobenzoate | 0.45 | 0.01 | 0.84 | 0.39 | 0.36 | 0.02 | -0.09 |
| 59 | 1219-38-1 | n-Octyl-4-hydroxybenzoate | 2.60 | 0.03 | 2.16 | -0.44 | 2.60 | 0.14 | 0.00 |
| 60 | 75-05-8 | Acetonitrile | -1.97 | na | -1.74 | 0.23 | -0.81 | 0.15 | 1.16 |
| 61 | 109-74-0 | Butyronitrile | -0.90 | 0.01 | -0.72 | 0.18 | -0.94 | 0.02 | -0.04 |
| 62 | 104-85-8 | p-Tolunitrile | 0.84 | 0.01 | 0.93 | 0.09 | 0.79 | 0.01 | -0.05 |
| 63 | 2243-27-8 | 1-Nonanenitrile | 1.99 | 0.02 | 1.99 | 0.00 | 1.95 | 0.02 | -0.04 |
| 64 | 75-52-5 | Nitromethane | -1.78 | 0.01 | -1.68 | 0.10 | -1.83 | 0.02 | -0.05 |
| 65 | 100-17-4 | 4-Nitroanisole | 0.81 | 0.01 | 0.97 | 0.16 | 0.80 | 0.01 | -0.01 |
| 66 | 121-14-2 | 2,4-Dinitrotoluene | 0.70 | 0.01 | 0.76 | 0.06 | 0.69 | 0.01 | -0.01 |
| 67 | 51-28-5 | 2,4-Dinitrophenol | -0.12 | 0.01 | -0.02 | 0.10 | -0.12 | 0.03 | 0.00 |
| 68 | 20651-71-2 | 4-Butylbenzoic acid | 1.74 | 0.03 | 0.86 | -0.88 | 1.71 | 0.06 | -0.03 |
| 69 | 2051-62-9 | 4-Chlorobiphenyl | 4.11 | 0.03 | 4.28 | 0.17 | 4.07 | 0.10 | -0.04 |
| 70 | 95-48-7 | o-Cresol | -0.65 | 0.02 | -0.72 | -0.07 | -0.75 | 0.02 | -0.10 |

(*continued on next page*)

**Table 2** (*continued*)

| ID | CAS | Compound | Measured $\log \mathbf{K}_{\mathbf{i,LDPE/W}}$(1) | SD | LSER[b] calc $\log \mathbf{K}_{\mathbf{i,LDPE/W}}$ (2) | Diff (2) – (1) | Measured $\log \mathbf{K}_{\mathbf{i,LDPEpris/W}}$(3) | SD | Diff (3) – (1) |
|---|---|---|---|---|---|---|---|---|---|
| 71 | 98-54-4 | 4-tert.-Butylphenol | 0.35 | 0.02 | 0.70 | 0.35 | 0.33 | 0.03 | -0.02 |
| 72 | 96-76-4 | 2,4-Di-tert.-butylphenol | 2.56 | 0.02 | 2.72 | 0.16 | 2.48 | 0.00 | -0.08 |
| 73 | 533-58-4 | 2-Iodophenol | 0.40 | 0.00 | 0.61 | 0.21 | 0.39 | 0.01 | -0.01 |
| 74 | 80-05-7 | Bisphenol A | -1.33 | 0.01 | -1.12 | 0.21 | -1.49 | 0.05 | -0.16 |
| 75 | 118-79-6 | 2,4,6-Tribromophenol | 2.30 | 0.01 | 2.07 | -0.23 | 2.28 | 0.02 | -0.02 |
| 76 | 115-86-6 | Triphenyl phosphate | 2.73 | 0.03 | 3.03 | 0.30 | 2.63 | 0.02 | -0.10 |
| 77 | 131-11-3 | Dimethyl phthalate | -0.13 | 0.02 | -0.37 | -0.24 | -0.20 | 0.02 | -0.07 |
| 78 | 84-66-2 | Diethyl phthalate | 0.77 | 0.01 | 0.68 | -0.09 | 0.75 | 0.01 | -0.02 |
| 79 | 84-74-2 | Dibutyl phthalate | 3.12 | 0.04 | 2.93 | -0.19 | 3.04 | 0.01 | -0.08 |
| 80 | 91-20-3 | Naphthalene | 2.82 | 0.02 | 2.80 | -0.02 | 2.79 | 0.01 | -0.03 |
| 81 | 83-32-9 | Acenaphthene | 3.61 | 0.02 | 3.47 | -0.14 | 3.59 | 0.01 | -0.02 |
| 82 | 129-00-0 | Pyrene | 4.86 | 0.03 | 4.76 | -0.10 | 4.83 | 0.09 | -0.03 |

[a]calculated by Eq. 13

[b]Note that sorption of the linear Aldehydes: 1-Butanal, 1-Hexanal and 1-Nonanal to purified LDPE showed pronounced deviation from the LSER calculated values and as well from values on pristine LDPE. These values were excluded for calculation of the LSER model specified by Eq. 13

from other studies. The literature set was further complemented by 3 Nitro-PNAs as reported by (Belles et al., 2016).

The total set of compounds spanned a wide range of chemical diversity and physicochemical properties: Relative molecular weight (Mr): 32 (Methanol) to 722 (2,2′,3,4,4′,5′,6-heptabromodiphenylether (BDE 183), log $K_{i,o/w}$: -0.72 (Methanol) to 8.61 (2,2′,3,4,4′,5′,6-heptabromodiphenylether (BDE 183) and $\log K_{i,LDPE/W}$: -3.35 (Methanol) up to 8.36 (n-dodecylbenzene). For all compounds (n=153), experimental solute descriptors could be retrieved from the UFZ LSER database.

With the distribution of the experimental values for $\log K_{i,LDPE/W}$ for the full data set shown in Fig. 1A, distribution of the test solute's associated descriptors is visualized in Fig. 1B. Histograms for the distribution of the specific solute descriptors in the test set can be found Fig. SI 2 of the SI.

Multicollinearity, i.e. correlation between a specific descriptor and the remaining descriptors presents a common challenge with MLR. As a measure for multicollinearity, the variance inflation factors (VIF) of the descriptor sets (full set and calibration set) were all found to range below a value of 5 for the LSER models of type "EV", thus providing evidence for acceptable multicollinearity. Descriptor sets for the LSER models of type "VL", both for experimental and QSPR-based descriptors exhibited multicollinearity caused by an inherently high cross-correlation of the V- and the L- descriptors (see Table SI 3 and Table SI 4 of SI along with detailed statistics of the LSER models). As these models were primarily constructed to allow comparison to the model of (Reppas-Chrysovitsinos et al., 2016) in part II of this article, no action was taken to mitigate multicollinearity within the sets submitted to MLR.

Results of the triplicate measurements of partition coefficients between LDPE (purified and pristine) and water were highly repeatable with mean standard deviations for purified LDPE: 0.026 ± 0.008 and pristine LDPE: 0.026 ± 0.016 (SDs reported in Table 2.) Mass balances for the batch sorption experiments ranged from 50 - 110 %, mean = 84% for purified LDPE and 50 - 115 %, mean = 86% for pristine LDPE. Measured values with mass balances ranging below 60% (volatiles 50%) were not reported and excluded from model calibration. For all batch experimental setups in this study, $\log K_{i,LDPE/W}$ values obtained for films of 50 μm and 200 μm thickness were essentially identical, thus providing proof that equilibrium was attained.

Overall, the batch equilibrium sorption method was considered well-suited for the objective of this study, i.e. the measurement of partition coefficients for a large set of test solutes and fulfilling the quality criteria specified above. Up to 10 compounds could be analyzed by one sample batch (triplicate measurements). Difficulties with measurement of highly volatile compounds were encountered, probably due to losses by volatilization at different steps in the procedure (results not reported).

### 3.2. *Impact of Calibration Solutes Molecular Features on Predictivity of Log - Linear Model for* $\log \mathbf{K}_{\mathbf{i,LDPE/W}}$

A plot of the full set of experimental values for $\log K_{i,LDPE/W}$ against $\log K_{i,O/W}$ is shown in Fig. 2. An initial inspection of the plot revealed, that while a collective of rather nonpolar compounds exhibits limited scatter around their attributed linear regression line, monopolar and bipolar compounds mostly reside distinctly below that regression line.

Monopolar compounds are characterized by their potential to act as either hydrogen bond donors (HDs) or hydrogen bond acceptors (HAs) while bipolar compounds exhibit both hydrogen bond donor and -acceptor potential. To facilitate separate statistical treatment on nonpolar (weak HDs/HAs) as opposed to monopolar (either strong HDs or HAs) and bipolar compounds (strong HDs and HAs), the identification of respective numerical upper limits for both the A- and B-descriptor ($UL_A$ and $UL_B$) respectively, was sought. This was achieved by successively decreasing $UL_A$ and $UL_B$ in steps of 0.01 (A-descriptor) and 0.1 (B-descriptor), respectively, starting at the maxima of the distributions. Compounds with A/B values exceeding the limits set were excluded from the linear regression. This iteration was continued until statistics ($R^2$, RMSE) of the linear regression for the remaining compounds then designated "weak HD/HA" (nonpolar) did not markedly improve. This procedure resulted in upper limits of $UL_A = 0.09$ and $UL_B = 0.6$. From the test solute set (n = 153), 26 compounds showed A-descriptors ≥ 0.09 and were consequently attributed be strong HDs. Analogously, 8 compounds with B-descriptors ≥ 0.6 were classified as strong HAs and 7 compounds were found to be both strong HDs and HAs.

The remaining compounds were classified as "weak HD/ HA" (Table SI 2).

Then, separate log-linear models were fitted as follows: First, regression of $\log K_{i,LDPE/W}$ for the full set of observations against $\log K_{i,O/W}$ yielded:

$$\log K_{i,LDPE/W} = 1.26(0.03)\cdot\log K_{i,O/W} - 1.99(0.12)$$
$$n = 156, R^2 = 0.930, RMSE = 0.742, F = 2040 \quad (11)$$

Second, consideration of compounds ascribed to "weak HD/HA" (nonpolar) only, resulted in:

$$\log K_{i,LDPE/W} = 1.18\ (0.01)\ \cdot\log K_{i,O/W} - 1.33(0.07)$$
$$n = 115, R^2 = 0.984, RMSE = 0.313, F = 7046 \quad (12)$$

Depicted in Fig. 2, a superior correlation was obtained in absence of either strong HDs and/or HAs. Values for these strong HDs/HAs exhibit a pronounced deviation from a regression line which was constructed for nonpolar compounds only. In essence, this observation corroborates earlier findings, e.g. (Goss, 2003) that is, a single parameter log-linear correlation to estimate partitioning between octanol and water is inappropriate when applied across multiple chemical classes or types of

**Table 3**
Literature data for $\log K_{i,LDPE/W}$ ($L_{water}$ / $L_{LDPE}$) near 25°C

| ID | CAS-RN | Compound | Experim.[a] $\log \mathbf{K}_{i,LDPE/W}$ (1) | LSER calc. $\log \mathbf{K}_{i,LDPE/W}$ (2) | Diff. (2) – (1) |
|---|---|---|---|---|---|
| 83 | 109-66-0 | Pentane | 2.72 | 2.00 | -0.72 |
| 84 | 110-54-3 | n-Hexane | 2.83 | 3.18 | 0.35 |
| 85 | 91-20-3 | Naphthalene | 3.04 | 2.80 | -0.24 |
| 86 | 83-32-9 | Acenaphthene | 3.70 | 3.47 | -0.23 |
| 87 | 208-96-8 | Acenaphthylene | 3.45 | 3.26 | -0.19 |
| 88 | 86-73-7 | Fluorene | 3.78 | 3.69 | -0.09 |
| 89 | 85-01-8 | Phenanthrene | 4.18 | 4.17 | -0.01 |
| 90 | 120-12-7 | Anthracene | 4.29 | 4.26 | -0.03 |
| 91 | 129-00-0 | Pyrene | 4.96 | 4.76 | -0.20 |
| 92 | 206-44-0 | Fluoranthene | 4.84 | 4.72 | -0.12 |
| 93 | 218-01-9 | Chrysene | 5.66 | 5.67 | 0.01 |
| 94 | 56-55-3 | Benz[a]anthracene | 5.67 | 5.67 | 0.00 |
| 95 | 207-08-9 | Benzo(k)fluoranthene | 6.30 | 6.07 | -0.23 |
| 96 | 192-97-2 | Benzo[e]pyrene | 6.12 | 5.65 | -0.47 |
| 97 | 205-99-2 | Benzo[b]fluoranthene | 6.30 | 5.89 | -0.41 |
| 98 | 198-55-0 | Perylene | 6.33 | 6.06 | -0.27 |
| 99 | 191-24-2 | Benzo(ghi)perylene | 6.93 | 7.00 | 0.07 |
| 100 | 53-70-3 | Dibenz[a,h]anthracene | 7.12 | 7.17 | 0.05 |
| 101 | 91-57-6 | 2-Methylnaphthalene | 3.45 | 3.25 | -0.20 |
| 102 | 571-58-4 | 1,4-dimethylnaphthalene | 3.75 | 3.84 | 0.09 |
| 103 | 569-41-5 | 1,8-dimethylnaphthalene | 3.65 | 3.78 | 0.13 |
| 104 | 2245-38-7 | 2,3,5-trimethylnaphthalene | 4.36 | 4.23 | -0.13 |
| 105 | 1730-37-6 | 1-methylfluorene | 4.11 | 4.23 | 0.12 |
| 106 | 13764-18-6 | 1,4,6,7-tetramethylnaphthalene | 4.78 | 4.76 | -0.02 |
| 107 | 2531-84-2 | 2-methylphenanthrene | 4.70 | 4.65 | -0.05 |
| 108 | 20928-02-3 | 2-Methyldibenzothiophene | 4.70 | 4.76 | 0.06 |
| 109 | 31317-14-3 | 1,2-Dimethydibenzothiophene | 4.89 | 5.23 | 0.34 |
| 110 | 575-41-7 | 1,3-Dimethylnaphthalene | 3.79 | 3.77 | -0.02 |
| 111 | 1576-67-6 | 3,6-Dimethylphenanthrene | 5.17 | 5.12 | -0.05 |
| 112 | 2381-21-7 | 1-Methylpyrene | 5.54 | 5.42 | -0.12 |
| 113 | 1705-85-7 | 6-Methylchrysene | 5.90 | 6.08 | 0.18 |
| 114 | 57-97-6 | 7,12-Dimethylbenz[a]anthracene | 6.35 | 6.75 | 0.40 |
| 115 | 2051-62-9 | 4-Chlorobiphenyl | 4.23 | 4.28 | 0.05 |
| 116 | 16605-91-7 | 2,3-Dichlorobiphenyl | 4.53 | 4.66 | 0.13 |
| 117 | 37680-65-2 | 2,2′,5-Trichlorobiphenyl | 4.90 | 5.08 | 0.18 |
| 118 | 55702-45-9 | 2,3,6-Trichlorbiphenyl | 5.46 | 5.08 | -0.38 |
| 119 | 16606-02-3 | 2,4′,5-Trichlorbiphenyl | 5.26 | 5.22 | -0.04 |
| 120 | 41464-39-5 | 2,2′,3,5′-Tetrachlorobiphenyl | 5.46 | 5.61 | 0.15 |
| 121 | 41464-43-1 | 2,3,3′,4′-Tetrachlorbiphenyl | 5.86 | 5.76 | -0.10 |
| 122 | 32598-13-3 | 3,3′,4,4′-Tetrachlorobiphenyl | 6.04 | 5.90 | -0.14 |
| 123 | 33284-52-5 | 3,3′,5,5′-Tetrachlorbiphenyl | 6.31 | 5.92 | -0.39 |
| 124 | 38380-02-8 | 2,2′,3,4,5′-Pentachlorobiphenyl | 6.16 | 6.13 | -0.03 |
| 125 | 38380-01-7 | 2,2′,4,4′,5-Pentachlorbiphenyl | 6.27 | 6.12 | -0.15 |
| 126 | 56558-16-8 | 2,2′,4,6,6′-Pentachlorobiphenyl | 5.96 | 6.06 | 0.10 |
| 127 | 65510-44-3 | 2,3′,4,4′,5′-Pentachlorbiphenyl | 6.42 | 6.27 | -0.15 |
| 128 | 38380-07-3 | 2,2′,3,3′,4,4′-Hexachlorbiphenyl | 6.59 | 6.65 | 0.06 |
| 129 | 38411-22-2 | 2,2′,3,3′,6,6′-Hexachlorbiphenyl | 6.74 | 6.61 | -0.13 |
| 130 | 35065-28-2 | 2,2′,3,4,4′,5′-Hexachlorobiphenyl | 6.50 | 6.65 | 0.15 |
| 131 | 35065-27-1 | 2,2′,4,4′,5,5′-Hexachlorobiphenyl | 6.67 | 6.65 | -0.02 |
| 132 | 38380-08-4 | 2,3,3′,4,4′,5-Hexachlorobiphenyl | 6.96 | 6.81 | -0.15 |
| 133 | 35065-30-6 | 2,2′,3,3′,4,4′,5-Heptachlorbiphenyl | 7.06 | 7.18 | 0.12 |
| 134 | 52663-68-0 | 2,2′,3,4′,5,5′,6-Heptachlorbiphenyl | 6.91 | 7.16 | 0.25 |
| 135 | 74472-52-9 | 2,2′,3,4,4′,5,6,6′-Octachlorbiphenyl | 7.69 | 7.80 | 0.11 |
| 136 | 52663-77-1 | 2,2′,3,3′,4,5,5′,6,6′-Nonachlorbiphenyl | 7.62 | 8.23 | 0.61 |
| 137 | 108-88-3 | Toluene | 1.98 | 2.00 | 0.02 |
| 138 | 95-47-6 | o-Xylene | 2.61 | 2.46 | -0.15 |
| 139 | 100-41-4 | Ethylbenzene | 2.48 | 2.53 | 0.05 |
| 140 | 119-64-2 | Tetralin | 3.16 | 3.20 | 0.04 |
| 141 | nHBz | t-Pentylbenzene | 4.06 | 4.17 | 0.11 |
| 142 | 1078-71-3 | n-Peptylbenzene | 5.06 | 5.29 | 0.23 |
| 143 | 2189-60-8 | n-Octylbenzene | 5.96 | 5.83 | -0.13 |
| 144 | 1081-77-2 | n-Nonylbenzene | 6.76 | 6.38 | -0.38 |
| 145 | 104-72-3 | n-Decylbenzene | 7.06 | 6.94 | -0.12 |
| 146 | 123-01-3 | n-Dodecylbenzene | 8.36 | 8.03 | -0.33 |
| 147 | 1806-26-4 | n-Octylphenol | 3.60 | 3.04 | -0.56 |
| 148 | 41318-75-6 | 2,4-Dibromo-1-(4-bromophenoxy)benzene | 5.68 | 5.76 | 0.08 |
| 149 | 5436-43-1 | 2,2′4,4′-Tetrabromodiphenyl ether | 6.22 | 6.29 | 0.07 |
| 150 | 60348-60-9 | 2,2′,4,4′,5-Pentabromodiphenyl ether | 6.82 | 6.84 | 0.02 |
| 151 | 189084-64-8 | 2,2′,4,4′,6-Pentabromodiphenyl ether | 6.74 | 7.02 | 0.28 |
| 152 | 68631-49-2 | 2,2′,4,4′,5,5′-Hexabromodiphenyl ether | 7.30 | 7.52 | 0.22 |
| 153 | 207122-15-4 | 2,2,4,4,5,6- Hexabromodiphenyl ether | 7.46 | 7.54 | 0.08 |
| 154 | 207122-16-5 | 2,2′,3,4,4′,5′,6-Heptabromodiphenyl ether | 7.60 | 8.26 | 0.66 |
| 155 | 132-65-0 | Dibenzothiophene | 4.26 | 4.11 | -0.15 |
| 156 | 3380-34-5 | Triclosan | 3.30 | 2.35 | -0.95 |

(*continued on next page*)

**Table 3** (*continued*)

| ID | CAS-RN | Compound | Experim.[a]log$\mathbf{K}_{i,LDPE/W}$ (1) | LSER calc.log$\mathbf{K}_{i,LDPE/W}$ (2) | Diff. (2) – (1) |
|---|---|---|---|---|---|
| 157 | 86-57-7 | 1-Nitronaphthalene | 2.51 c | 2.31 | -0.20 |
| 158 | 581-89-5 | 2-Nitronaphthalene | 2.18 c | 2.54 | 0.36 |
| 159 | 5522-43-0 | 1-Nitropyrene | 4.81 c | 4.65 | -0.16 |

[a]values from (Liu et al., 2017)
[b]calculated by using Eq. 13
[c]values from (Belles et al., 2016)

Belles, A., Alary, C., Criquet, J., Billon, G., 2016. A new application of passive samplers as indicators of in-situ biodegradation processes. Chemosphere 164, 347-354.
Liu, H., Wei, M., Yang, X., Yin, C., He, X., 2017. Development of TLSER model and QSAR model for predicting partition coefficients of hydrophobic organic chemicals between low density polyethylene film and water. Sci. Total Environ. 574, 1371-1378.

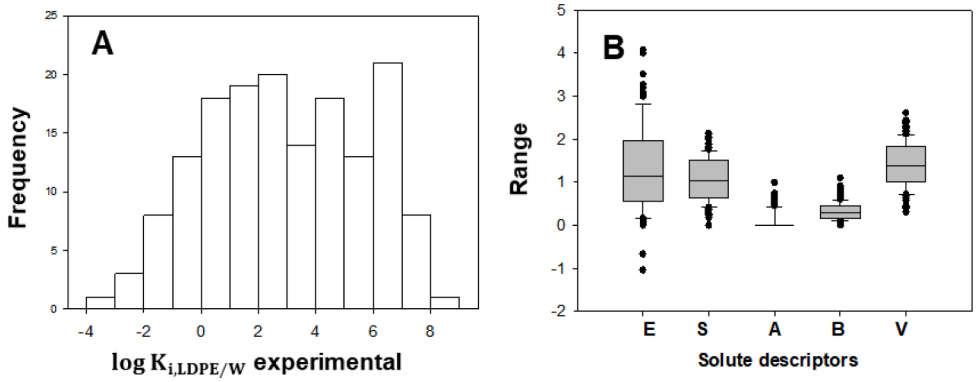


**Fig. 1.** Distribution of experimental values for log$K_{i,LDPE/W}$ (full solute set, n =153) (A); LSER solute descriptor distribution for experimental test set (full set, n = 153 solutes) (B)

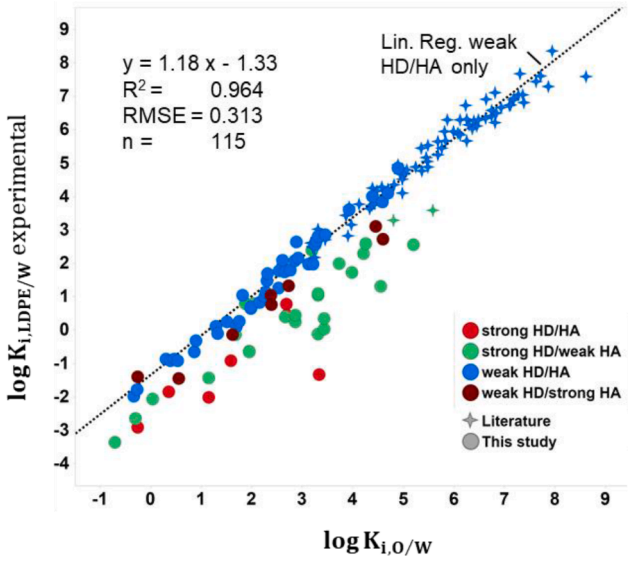


**Fig. 2.** Plot of experimental partition coefficients log$K_{i,LDPE/W}$ against log$K_{i,O/W}$. The linear regression line and parameters are calculated from values for weak hydrogen donors (HD) /-acceptors (HA), only.

potential molecular interactions exerted by a compound. The underlying reason is that for compounds undergoing specific, complementary interactions involving hydrogen-bond donor or – acceptor functionalities, octanol as a bipolar phase cannot simulate a purely nonpolar phase like a polyolefin. Vice versa, this finding is also indicative for the notion that a linear correlation to log$K_{i,O/W}$ (i.e. spLFER) could provide sufficient accuracy, as long as only nonpolar compounds and/or compounds exhibiting weak hydrogen bonding donor- and/or acceptor strength are involved.

### 3.3. *Calibration of LSER models for* log$\mathbf{K}_{i,LDPE/W}$

Fitting of experimental values for log$K_{i,LDPE/W}$ from the full data set to Eq. 6 yielded:

$$\log K_{i,LDPE/W} = -0.529 + 1.098\ E - 1.557\ S - 2.991\ A - 4.617\ B + 3.886\ V$$
$$n = 156, R^2 = 0.991, RMSE = 0.264, F = 3436 \quad (13)$$

Fig. 3 shows a plot of experimental log$K_{i,LDPE/W}$ versus values

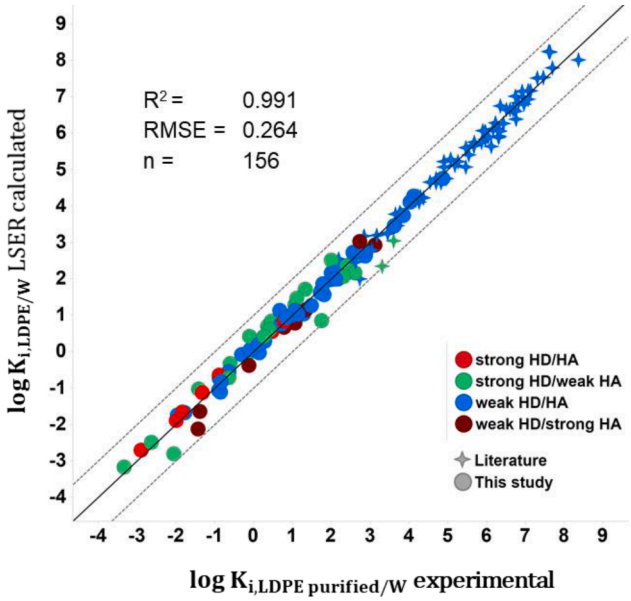


**Fig. 3.** Plot of LSER calculated partition coefficients log$K_{i,LDPE/W}$ (eq. (13)) versus experimental values - full set solute set, n =153. Solid line: 1:1 line. Dotted lines: ± 1 log unit.

predicted by the LSER(EV) model. A very good correlation was obtained ($R^2 = 0.991$). The RMSE of 0.264 is considered excellent but slightly higher than RMSEs typical for solvent/water partition systems (0.10 – 0.20). Of note, the three linear aldehydes in the test solute set (1-butanal, 1-hexanal, 1-nonanal), with no reasoning available, showed a systematic deviation from the 1:1 line and were therefore excluded from calibration of the model given by Eq. 13.

Fig. 4

Additionally, from partition coefficients for the full data set associated to compounds with an experimental L-descriptor available, a LSER (VL) model for use in part II of this work was fitted to Eq. 8.

$$\log K_{i,LDPE/W} = -0.330 - 1.512\ S_i - 3.396\ A_i - 5.069\ B_i + 2.115\ V_i + 0.594\ L_i$$
$$n = 138, R^2 = 0.988, RMSE = 0.308, F = 2237 \quad (14)$$

Further statistics associated to Eqn 13 and 14 are provided tables SI 3 and SI 4 in the SI.

### 3.4. Purified vs. pristine LDPE

All $\log K_{i,LDPE/W}$ values measured in this study were generated in parallel for samples of purified and pristine LDPE ($\log K_{i,LDPEpris/W}$). Overall, pristine LDPE produced slightly lower partition coefficients than purified LDPE with more pronounced differences in the lower $\log K_{i,LDPE/W}$ region, i. e. for more polar compounds (see Table 2). This observation might be attributed to the presence of an extractable fraction of low molecular oligomeric hydrocarbons in pristine (non-purified) LDPE exhibiting a somewhat higher potential for dispersive interactions and thus rendering pristine LDPE more apolar then the purified polymer backbone. In the literature, the composition of this extractable fraction is ascribed to a complex mixture of highly isomerized, branched alkanes and alkenes (see also section 1 of SI) (Biedermann-Brem et al., 2012). As the purification procedure might also affect the crystallinity of the material, no mechanistical reasoning is available to the authors, how this in turn might impact the materials sorption behavior to polar chemicals. Of note and yet with no reasoning available, all linear aldehydes in the test set (i. e. 1-butanal, 1-hexanal and 1-nonanal) showed a distinctly higher sorption into the purified material as (i) compared to the LSER predicted value and (ii) to the value for the pristine material.

## 4. CONCLUSION AND OUTLOOK

Partition coefficients LDPE/water for a broad set of chemically diverse chemicals could be successfully measured and complemented by experimental values from the literature. To a great deal, these compounds are also indicative for potentially leachable compounds encountered in plastics for pharmaceutical- and food contact use. The calibrated Abraham-type linear solvation energy relationships (LSERs) obtained from these partition coefficients were demonstrated to provide an accurate and robust means for the prediction of partition coefficients between LDPE and water, as proven by a coefficient of determination of 0.985 and a standard deviation of 0.352 for an independent validation set of the LSER(EV)-model (n = 52, see part II of this article).

Application of the models is straightforward, i.e. solute descriptors and corresponding system parameters can be easily retrieved from a publicly available database or, with some constraints in predictability, generated by a QSPR. Then, just by simple arithmetics, partition coefficients can be calculated and utilized for assessment of compound equilibrium levels in a polymer-contacting solution based on knowledge of the total compound pool. Here, this study, similar to previous reports, demonstrated that LSERs clearly outperform log-linear correlations to solvent/water systems as yet recommended for modeling of mass transport from plastics to aqueous based solutions.

Of note, LSERs were proven to be well-suited in accounting for the partition behavior of compounds exhibiting significant hydrogen-bonding donor or acceptor potential, i. e. mono- or bipolar compounds. The reason for that observation is that LSER descriptors, in contrast to $\log K_{i,O/W}$ as a single holistic lipophilicity parameter, carry additional information on the strength of specific potential molecular interactions a compound can undergo, in particular on its potential to act as hydrogen bonding acceptor or –donor, respectively. Notwithstanding, if only nonpolar compounds (weak HDs/HAs) are involved in a desired projection of partition coefficients, log-linear correlations to $\log K_{i,O/W}$ were demonstrated to represent a simple, albeit potentially sufficient, screening approach.

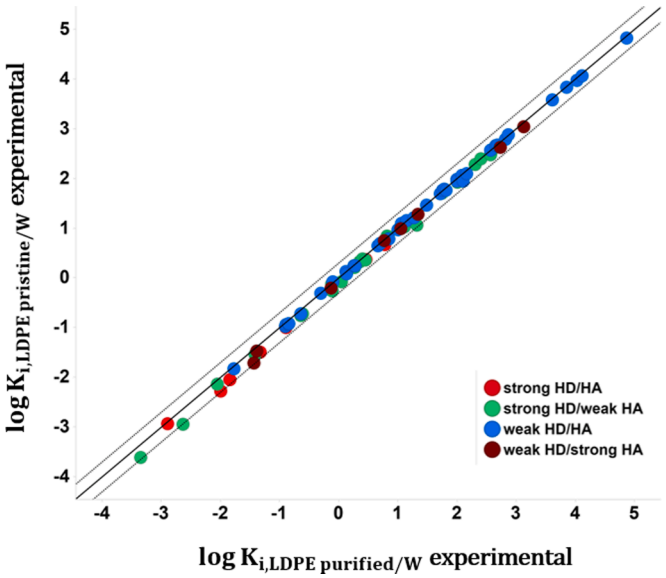


**Fig. 4.** Plot of experimental values from this study for $\log K_{i,LDPEpris/W}$ (pristine LDPE) vs. $\log K_{i,LDPE/W}$ (purified LDPE). Solid line: 1:1 line. Dotted lines: ± 0.3 log units. Partition coefficients of more polar compounds tend to be lower in pristine LDPE.

Overall, equilibrium partitioning of neutral solutes between LDPE and water was demonstrated a highly predictable process. Consequently, for migrants with $pK_A$ values ensuring negligible dissociation under the given conditions of pH, a reliable estimate of maximum levels in a contacting aqueous solution is possible if their total pool in the combined phases in known.

By comparison of partitioning data between pristine and purified LDPE samples, it became evident that that solvent extraction applied as a material purification process renders the material slightly less hydrophobic, i. e. polar compounds in particular tend to exhibit a little lower sorption into the pristine material with differences in $\log K_{i,LDPE/W}$ up to about 0.3 log units. This might be caused by the presence of low molecular fractions of hydrocarbons in the pristine polymer.

A more in-depth evaluation of the LSER models predictivity along with a comparison to data and models from the literature is provided in part II of this work.

### CRediT authorship contribution statement

**Thomas Egert:** Project administration, Conceptualization, Investigation, Methodology, Resources, Data curation, Formal analysis, Validation, Visualization, Writing – original draft. **Horst-Christian Langowski:** Writing – review & editing, Supervision.

### Declaration of Competing Interest

The authors report no competing financial interest.

*ACKNOWLEDGEMENTS*

Kai-Uwe Goss and Nadin Ulrich, Helmholtz Centre for Environmental Research, Leipzig, are acknowledged for inspiring discussions and curation of LSER data. Polifilm Extrusion GmbH is thanked for providing the LDPE films.

*FUNDING STATEMENT*

This research was funded by Boehringer Ingelheim Pharma GmbH.

## Supplementary materials

Supplementary material associated with this article can be found, in the online version, at doi:10.1016/j.ejps.2022.106137.

## References

Abraham, M.H., Kamlet, M.J., Taft, R.W., 1982. Linear solvation energy relationships. Part 19. Correlation of the free energies of solution of 41 solutes in select solvents with hildebrand's solubility parameter, ÎH, and with the solvatochromic parameter Ïĉ, 923–928.

Abraham, M.H., McGowan, J.C., 1987. The use of characteristic volumes to measure cavity terms in reversed phase liquid chromatography. Chromatographia 23, 243–246.

Abraham, M.H., 1993. Scales of solute hydrogen-bonding: Their construction and application to physicochemical and biochemical processes. Chemical Society Reviews 22, 73–83.

Abraham, M.H., Ibrahim, A., Zissimos, A.M., 2004. Determination of sets of solute descriptors from chromatographic measurements. J. Chromatogr. A 1037, 29–47.

Begley, T., Castle, L., Feigenbaum, A., Franz, R., Hinrichs, K., Lickly, T., Mercea, P., Milana, M., O'Brien, A., Rebre, S., Rijk, R., Piringer, O., 2005. Evaluation of migration models that might be used in support of regulations for food-contact plastics. Food Addit. Contam. 22, 73–90.

Belles, A., Alary, C., Criquet, J., Billon, G., 2016. A new application of passive samplers as indicators of in-situ biodegradation processes. Chemosphere 164, 347–354.

Biedermann-Brem, S., Kasprick, N., Simat, T., Grob, K., 2012. Migration of polyolefin oligomeric saturated hydrocarbons (POSH) into food. Food Addit. Contam. Part A Chem. Anal. Control Exposure Risk Assess 29, 449–460.

Biophorum Operations Group (BPOG), 2017. Best Practices Guide for Evaluating Leachables Risk From Polymeric Single-Use Systems used in Biopharmaceutical Manufacturing.

Collander, R., 1951. The Partition of Organic Compounds Between Higher Alcohols and Water. Acta Chemica Scandinavica 5, 774–780.

Crank, J., 1975. The Mathematics of Diffusion. Oxford University Press, Ely House, London W.l. Second Edition ed.

Egert, T., 2018. Exploring Mass Transport Modeling (MTM) as a Critical Tool for Risk-Based E&L Study Designs: A Holistic Perspective. Smithers Extratables & Leachables USA, 2018.

Egert, T., Langowski, H.-C., 2022. Linear Solvation Energy Relationships (LSERs) for Accurate Prediction of Partition Coefficients between Low Density Polyethylene and Water - Part II: Model Evaluation and Benchmarking. Eur. J. Pharm. Sci. 172 (1), 1–10. https://doi.org/10.1016/j.ejps.2022.106138, 106138.

Reaxys®, ELSEVIER Life Sciences. https://www.reaxys.com/#/search/quick Last accessed: August 16, 2021.

Endo, S., Droge, S.T.J., Goss, K.U., 2011a. Polyparameter linear free energy models for polyacrylate fiber-water partition coefficients to evaluate the efficiency of solid-phase microextraction. Anal. Chem 83, 1394–1400.

Endo, S., Goss, K.U., 2014a. Applications of polyparameter linear free energy relationships in environmental chemistry. Environ. Sci. Technol 48, 12477–12491.

Endo, S., Goss, K.U., 2014b. Predicting partition coefficients of polyfluorinated and organosilicon compounds using polyparameter linear free energy relationships (PP-LFERs). Environ. Sci. Technol 48, 2776–2784.

Endo, S., Hale, S.E., Goss, K.U., Arp, H.P.H., 2011b. Equilibrium partition coefficients of diverse polar and nonpolar organic compounds to polyoxymethylene (POM) passive sampling devices. Environ. Sci. Technol. 45, 10124–10132.

European Medicines Agency (EMA), CPMP/QWP/4359/03, EMEA/CVMP/205/04, Guideline on Plastic Immediate Packaging Materials, 2005.

Commission Regulation (EU) No 10/2011 of 14 January 2011 on plastic materials and articles intended to come into contact with food, 2011.

Fang, X., Vitrac, O., 2017. Predicting diffusion coefficients of chemicals in and through packaging materials. Crit. Rev. Food Sci. Nutr. 57, 275–312.

Franz, R., 2005. Migration modeling from food-contact plastics into foodstuffs as a new tool for consumer exposure estimation. Food Addit. Contam. 22, 920–937.

Fick, A., 1855. About Diffusion. Ann. Phys. Chem. 94, 59–86.

Freedonia Group - Industry Market Research, 2018. Global Pharmaceutical Packaging. https://www.freedoniagroup.com/industry-study/world-pharmaceutical-packaging-3269.htm. Accessed: August 16, 2021.

Goss, K.U., 2003. The Octanol/Water Partitioning Coefficient - The Remedy of Environmental Chemistry? Umweltwissenschaften und Schadstoff-Forschung 15, 273–279.

Goss, K.U., 2005. Predicting the equilibrium partitioning of organic compounds using just one linear solvation energy relationship (LSER). Fluid Phase Equilib 233, 19–22.

Goss, Kai-Uwe, 2011. Using COSMO-RS for the Prediction of Vapor-Liquid Equilibria, Gas Solubilities and Partition Coefficients in Polymers. Analytical Chemistry 83 (13), 5304–5308. https://doi.org/10.1021/ac200733v.

Goss, K.U., Schwarzenbach, R.P., 2001. Linear free energy relationships used to evaluate equilibrium partitioning of organic compounds. Environ. Sci. Technol. 35, 1–9.

Guazzotti, Valeria, et al., 2021. Migration from acrylonitrile butadiene styrene (ABS) polymer: swelling effect of food simulants compared to real foods. Journal of Consumer Protection and Food Safety 16 (1), 19–33. https://doi.org/10.1007/s00003-020-01308-8.

Guo, X., et al., 2012. Sorption of four hydrophobic organic compounds by three chemically distinct polymers: Role of chemical and physical composition. Environmental Science and Technology 46 (13). https://doi.org/10.1021/es301386z, 7552–7259.

Hauk, A., Pahl, I., Dorey, S., Menzel, R., 2021. Using extractables data from single-use components for extrapolation to process equipment-related leachables: The toolbox and justifications. Eur. J. Pharm. Sci. 163.

Hayward, D.S., Kenley, R.A., Jenke, D.R., 1990. Interactions between polymer containers and parenteral solutions: the correlation of equilibrium constants for polymer-water partitioning with octanol-water partition coefficients. Int. J. Pharm. 59, 245–253.

Hoekstra, E.J.B.R.; Dequatre, C.; Mercea, P.; Milana, M.R.; Störmer, A.; Trier, X.; Vitrac, O.; Schäfer, A.; Simoneau, C., 2015. Practical Guidelines on the Application of Migration Modelling for the Estimation of Specific Migration.

Hüffer, T., Hofmann, T., 2016. Sorption of non-polar organic compounds by micro-sized plastic particles in aqueous solution. Environ. Pollut. 214, 194–201.

International Standardization Organisation (ISO), ISO 10993-18:2020 Biological evaluation of medical devices Part 18: Chemical characterization of medical device materials within a risk management process. 2020-01.

Jenke, D., 2011. A general assessment of the physicochemical factors that influence leachables accumulation in pharmaceutical drug products and related solutions. PDA Journal of Pharmaceutical Science and Technology 65, 166–176.

Jenke, D., 2017. Identification, analysis and safety assessment of leachables and extractables. TrAC Trends Anal. Chem.

Jenke, D., Barge, V.J., 2014. Mathematical modeling of the extractables release from multi-layered plastic films used in drug product containers. J. Appl. Polym. Sci.

Josefsson, S., Arp, H.P.H., Kleja, D.B., Enell, A., Lundstedt, S., 2015. Determination of polyoxymethylene (POM) - water partition coefficients for oxy-PAHs and PAHs. Chemosphere 119, 1268–1274.

Kubicova, Marie, et al., 2022. Styrene-acrylonitrile-copolymer and acrylonitrile-butadiene-styrene-copolymer: a study on extractable and migratable oligomers. Food Additives and Contaminants - Part A 39 (2), 397–414. https://doi.org/10.1080/19440049.2021.1995631.

Kühne, Frederike, et al., 2021. Characterisation of Elastomers as Food Contact Materials-Part 1: Quantification of Extractable Compounds, Swelling of Elastomers in Food Simulants and Release of Elements. Molecules 26 (2), 1–18. https://doi.org/10.3390/molecules26020509, 509.

Liu, H., Wei, M., Yang, X., Yin, C., He, X., 2017. Development of TLSER model and QSAR model for predicting partition coefficients of hydrophobic organic chemicals between low density polyethylene film and water. Sci. Total Environ. 574, 1371–1378.

Lützow, N., Tihminlioglu, A., Danner, R.P., Duda, J.L., De Haan, A., Warnier, G., Zielinski, J.M., 1999. Diffusion of toluene and n-heptane in polyethylenes of different crystallinity. Polymer 40, 2797–2803.

McPhedran, K.N., Seth, R., Drouillard, K.G., 2012. Investigation of effects of the cosolvent methanol on the apparent solubility of a suite of chlorobenzenes using headspace solid-phase microextraction (HS-SPME). J Chem Eng Data 57, 2373–2378.

Mercea, P.V., Kalisch, A., Ulrich, M., Benz, H., Piringer, O.G., Toşa, V., Schuster, R., Sejersen, P., 2019. Modelling migration of substances from polymers into drinking water. Part 2 – Partition coefficient estimations. Polym Test 76, 420–432.

Paudel, K., Hauk, A., Maier, T.V., Menzel, R., 2020. Quantitative characterization of leachables sinks in biopharmaceutical downstream processing. Eur. J. Pharm. Sci. 143, 105069.

Pintado-Herrera, M.G., Lara-Martin, P.A., Gonzalez-Mazo, E., Allan, I.J., 2016. Determination of silicone rubber and low density polyethylene diffusion and polymer-water partition coefficients for emerging contaminants. Environ Toxicol Chem.

Poole, C.F., Atapattu, S.N., Poole, S.K., Bell, A.K., 2009. Determination of solute descriptors by chromatographic methods. Anal. Chim. Acta 652, 32–53.

Product Quality and Research Institute (PQRI), 2006. Safety Thresholds and Best Practices for Extractables and Leachables in Orally Inhaled and Nasal Drug Products. September 8.

Reppas-Chrysovitsinos, E., Sobek, A., MacLeod, M., 2016. Screening-level models to estimate partition ratios of organic chemicals between polymeric materials, air and water. Environ. Sci. Process. Impacts 18, 667–676.

Feigenbaum, A.E., Riquet, A.M., Scholler, D., 2000. Fatty food simulants: Solvents to mimic the behavior of fats in contact with packaging plastics, pp. 71–81, 753 ed.

Saylor, D.M., Chandrasekar, V., Simon, D.D., Turner, P., Markley, L.C., Hood, A.M., 2019. Strategies for Rapid Risk Assessment of Color Additives Used in Medical Devices. Toxicol. Sci. 172, 201–212.

Smithers, 2019. The Future of Rigid Plastic Packaging to 2024. Akron, OH, USA.

Sprunger, L., Proctor, A., Acree, J., Abraham, M.H., 2007. Characterization of the sorption of gaseous and organic solutes onto polydimethyl siloxane solid-phase microextraction surfaces using the Abraham model. J. Chromatogr. A 1175, 162–173.

Taft, R.W., Abboud, J.L.M., Kamlet, M.J., Abraham, M.H., 1985. Linear solvation energy relations. J Solution Chem 14, 153–186.

EPI SuiteTM (Estimation Programs Interface v4.11), U.S. Environmental Protection Agency. https://www.epa.gov/tsca-screening-tools/download-epi-suitetm-estimation-program-interface-v411 Last accessed: August 16, 2021.

U.S. Food and Drug Administration (FDA), Guidance for Industry: Container Closure Systems for Packaging Human Drugs and Biologics (Chemistry, Manufacturing, and Controls Documentation), 1999.

Uber, Tobias H., 2019. Sorption of non-ionic organic compounds by polystyrene in water. Science of the Total Environment 682, 348–355. https://doi.org/10.1016/j.scitotenv.2019.05.040.

Ulrich, N., Endo, S., Brown, T.N., Watanabe, N., Bronner, G., Abraham, M.H., Goss, K.U., 2017. UFZ-LSER database v 3.2.

United States Food and Drug (FDA), Guidance for Industry - Preparation of Premarket Submissions for Food Contact Substances (Chemistry Recommendations), 2007.

United States Pharmacopoeia (USP), <661>Plastic Containers. USP 35 - NF 30, Official as of 1-Dec-2015.

United States Pharmacopoeia (USP), <1663>Assessment of Extractables associated with Pharmaceutical Packaging/Delivery Systems. USP 41 - NF 36, Official as of 1-Dec-2020.

United States Pharmacopoeia (USP), <1664>Assessment of Drug Product Leachables Associated with Pharmaceutical Packaging Delivery Systems. USP 41 - NF 36, Official as of 1-Dec-2020.

Vitha, M., Carr, P.W., 2006. The chemical interpretation and practice of linear solvation energy relationships in chromatography. J. CHROMATOGR. A 1126 (1–2), 143–194. https://doi.org/10.1016/j.chroma.2006.06.074.

Welle, F., 2014. Activation energies of diffusion of organic migrants in cyclo olefin polymer. Int. J. Pharm 473, 510–517.